

# **Seasonal Dynamics of Epiphytic Microbial Communities on Marine Macrophyte Surfaces**

Marino Korlević<sup>1\*</sup>, Marsej Markovski<sup>1</sup>, Zihao Zhao<sup>2</sup>, Gerhard J. Herndl<sup>2,3</sup>, Mirjana Najdek<sup>1</sup>

1. Center for Marine Research, Ruđer Bošković Institute, Croatia

2. Department of Functional and Evolutionary Ecology, University of Vienna, Austria

3. Department of Marine Microbiology and Biogeochemistry, Royal Netherlands Institute for Sea Research, Utrecht University, The Netherlands

\*To whom correspondence should be addressed:

Marino Korlević

G. Paliaga 5, 52210 Rovinj, Croatia

Tel.: +385 52 804 768

Fax: +385 52 804 780

e-mail: [marino.korlevic@irb.hr](mailto:marino.korlevic@irb.hr)

Running title: Seasonal dynamics of epiphytic communities

## 1 Summary

2 Surfaces of marine macrophytes (seagrasses and macroalgae) are inhabited by diverse  
3 microbial communities. Most studies focusing on macrophyte epiphytic communities did not  
4 take into account temporal changes or applied low sampling frequency approaches. Illumina  
5 sequencing of the V4 16S rRNA region was performed to determine the seasonal dynamics  
6 of epiphytic communities sampled from the surfaces of the seagrass *Cymodocea nodosa* and  
7 invasive macroalga *Caulerpa cylindracea*. Leaves and thalli were sampled in a meadow of  
8 *Cymodocea nodosa* invaded by the invasive *Caulerpa cylindracea* and in a monospecific  
9 settlement of *Caulerpa cylindracea* located in the proximity of the meadow at monthly intervals.  
10 For comparison the ambient prokaryotic plankton community was also characterized. Sequencing  
11 results at the OTU level showed a clear differentiation between ambient water and epiphytic  
12 communities and a host-specific community assemblage. In addition, successional changes were  
13 observed that could be connected to the macrophyte growth cycle. Taxonomic analysis showed  
14 similar high rank groups in the ambient water and epiphytic communities, with the exception of  
15 *Desulfobacterota* that were found only on *Caulerpa cylindracea*. Only *Cyanobacteria* showed  
16 seasonal change, while other high rank taxa were present throughout the year. In every analyzed  
17 high rank taxa, phylogenetic groups present throughout the year comprised most of the sequences  
18 and could be identified together with low proportion taxa showing seasonal patterns connected to  
19 the macrophyte growth cycle. Taken together, epiphytic microbial communities of the seagrass  
20 *Cymodocea nodosa* and the macroalgae *Caulerpa cylindracea* appear to be host-specific and  
21 contain taxa that undergo successional changes.

22 **Introduction**

23       Marine macrophytes (seagrasses and macroalgae) are important ecosystem engineers that  
24   form close associations with microorganism belonging to all three domains of life (Egan *et al.*,  
25   2013; Tarquinio *et al.*, 2019). Microbes can live within macrophyte tissue as endophytes or can  
26   form epiphytic communities on surfaces of leaves and thalli (Egan *et al.*, 2013; Hollants *et al.*,  
27   2013; Tarquinio *et al.*, 2019). Epiphytic and endophytic microbial communities form a close  
28   functional relationship with the macrophyte host. It was proposed that this close relationship  
29   constitutes a holobiont, an integrated community where the macrophyte organism and its symbiotic  
30   partners support each other (Margulis, 1991; Egan *et al.*, 2013; Tarquinio *et al.*, 2019).

31       Biofilms formed from microbial epiphytes can contain diverse taxonomic groups and harbor  
32   cell densities from  $10^2$  to  $10^7$  cells  $\text{cm}^{-2}$  (Armstrong *et al.*, 2000; Bengtsson *et al.*, 2010; Burke  
33   and Thomas *et al.*, 2011). In such an environment a number of positive and negative interactions  
34   between the macrophyte and colonizing microorganisms have been described (Egan *et al.*, 2013;  
35   Hollants *et al.*, 2013; Tarquinio *et al.*, 2019). Macrophytes can promote growth of associated  
36   microbes by nutrient exudation, while in return microorganisms may support macrophyte  
37   performance through improved nutrient availability, phytohormone production and protection  
38   from toxic compounds, oxidative stress, biofouling organisms and pathogens (Egan *et al.*, 2013;  
39   Hollants *et al.*, 2013; Tarquinio *et al.*, 2019). Beside this positive interactions, macrophytes can  
40   negatively impact the associated microbes such as pathogenic bacteria by producing reactive  
41   oxygen species and secondary metabolites (Egan *et al.*, 2013; Hollants *et al.*, 2013; Tarquinio *et*  
42   *al.*, 2019).

43       All these ecological roles are carried out by a taxonomically diverse community of  
44   microorganisms. At higher taxonomic ranks a core set of macrophyte epiphytic taxa was  
45   described consisting mainly of *Alphaproteobacteria*, *Gammaproteobacteria*, *Desulfobacterota*,  
46   *Bacteroidota*, *Cyanobacteria*, *Actinobacteriota*, *Firmicutes*, *Planctomycetota*, *Chloroflexi* and

47 *Verrucomicrobiota* (Crump and Koch, 2008; Tujula *et al.*, 2010; Lachnit *et al.*, 2011). In contrast,  
48 at lower taxonomic ranks host specific microbial communities were described (Lachnit *et al.*,  
49 2011; Roth-Schulze *et al.*, 2016). Recently, it was shown that even different morphological niches  
50 within the same alga had a higher influence on bacterial community variation than biogeography  
51 or environmental factors (Morrissey *et al.*, 2019). While there is high community variation  
52 between host species it was observed that the majority of metagenome determined functions were  
53 conserved both between host species and individuals (Burke and Peter Steinberg *et al.*, 2011;  
54 Roth-Schulze *et al.*, 2016). This discrepancy between taxonomic and functional composition  
55 could be explained by the lottery hypothesis. It postulates that an initial random colonization step  
56 is performed from a set of functionally equivalent taxonomic groups resulting in taxonomically  
57 different epiphytic communities sharing a core set of functional genes (Burke and Peter Steinberg  
58 *et al.*, 2011; Roth-Schulze *et al.*, 2016). In addition, some of the variation in the observed data  
59 could be attributed to different techniques used in various studies, such as different protocols  
60 for epiphytic cell detachment and/or DNA isolation, as no standard protocol to study epiphytic  
61 communities was established (Ugarelli *et al.*, 2019; Korlević *et al.*, 2020, submitted).

62 The majority of studies describing macrophyte epiphytic communities did not encompass  
63 seasonal changes (Crump and Koch, 2008; Lachnit *et al.*, 2009; Burke and Thomas *et al.*, 2011;  
64 Roth-Schulze *et al.*, 2016; Ugarelli *et al.*, 2019). In addition, if seasonal changes were taken into  
65 account low temporal frequency and/or methodologies that do not allow high taxonomic resolution  
66 were used (Tujula *et al.*, 2010; Lachnit *et al.*, 2011; Miranda *et al.*, 2013; Michelou *et al.*, 2013).  
67 In the present study we describe the seasonal dynamics of bacterial and archaeal communities on  
68 the surfaces of the seagrass *Cymodocea nodosa* and siphonous macroalgae *Caulerpa cylindracea*  
69 determined on a mostly monthly scale. Bacterial and archaeal epiphytes were sampled in a meadow  
70 of *C. nodosa* invaded by the invasive *C. cylindracea* and in a locality of only *C. cylindracea*  
71 located in the proximity of the meadow. In addition, for comparison, the community of the ambient  
72 seawater was characterized.

73 **Results**

74 Sequencing of the 16S rRNA V4 region yielded a total of 1.8 million sequences after  
75 quality curation and exclusion of eukaryotic, chloroplast, mitochondrial and no relative sequences  
76 (Table S1). A total of 35 samples originating from epiphytic archaeal and bacterial communities  
77 associated with surfaces of the seagrass *C. nodosa* and macroalga *C. cylindracea* were analyzed. In  
78 addition, 18 samples (one of the samples was sequenced two times) originating from picoplankton  
79 archaeal and bacterial communities in the ambient seawater were also processed for comparison.  
80 The number of reads per sample ranged between 8,408 and 77,463 sequences (Table S1). Even  
81 when the highest sequencing effort was applied the rarefaction curves did not level off that is a  
82 common observation in high-throughput 16S rRNA amplicon sequencing approaches (Fig. S1).  
83 Following quality curation and exclusion of sequences mentioned before reads were clustered  
84 into 28,750 different OTUs at a similarity level of 97 %. Read numbers were normalized to the  
85 minimum number of sequences, 8,408 (Table S1), through rarefaction resulting in 17,196 different  
86 OTUs that ranged from 371 to 2,070 OTUs per sample (Fig. S2). To determine seasonal changes of  
87 richness and diversity the Observed Number of OTUs, Chao1, ACE, Exponential Shannon (Jost,  
88 2006) and Inverse Simpson were calculated after normalization through rarefaction. Generally,  
89 richness estimators and diversity indices showed similar trends. On average, higher values were  
90 found for *C. cylindracea* (mixed [Number of OTUs,  $1,694.9 \pm 130.8$  OTUs] and monospecific  
91 [Number of OTUs,  $1,737.2 \pm 171.4$  OTUs]), middle values for *C. nodosa* (Number of OTUs,  
92  $1,056.2 \pm 209.3$  OTUs) and lower values for picoplankton communities in the ambient seawater  
93 (Number of OTUs,  $527.4 \pm 147.5$  OTUs) (Fig. S2). Seasonal changes did not show such large  
94 dissimilarities. *C. nodosa* communities showed a slow increase towards the end of the study,  
95 while *C. cylindracea* (mixed and monospecific) communities were characterized by slightly larger  
96 values in Spring and Summer in comparison to Autumn and Winter (Fig. S2).

97 To determine the proportion of shared archaeal and bacterial OTUs and communities  
98 sampled in different environments the Jaccard's Similarity Coefficient on presence-absence

99 data and Bray-Curtis Similarity Coefficient were, respectively, calculated. Coefficients were  
100 determined after normalization through rarefaction and binning of samples from a particular  
101 environment. The highest proportion of shared OTUs and community was found between mixed  
102 and monospecific *C. cylindracea* (Jaccard, 0.35; Bray-Curtis, 0.78), while lower shared values  
103 were calculated between seawater and epiphytic communities (Fig. 1). Shared proportion between  
104 *C. nodosa* and *C. cylindracea* were approximately in the middle between these two extremes. To  
105 assess seasonal changes in the proportion of shared OTUs and communities the Jaccard's and  
106 Bray-Curtis Similarity Coefficients were calculated between consecutive sampling points (Fig. 2).  
107 Both coefficients showed similar trends. Temporal proportional changes were more pronounced  
108 for seawater in comparison to *C. nodosa* and especially *C. cylindracea* associated communities  
109 (Fig. 2). In addition, only 0.4 – 1.0 % of OTUs from each surface associated community were  
110 found at every time point. These OTUs also made a high proportion of total sequences (41.3 – 52.5  
111 %). To further disentangle the environmental and seasonal community dissimilarity a Principal  
112 Coordinates Analysis (PCoA) based on Bray-Curtis distances and OTU abundances was applied.  
113 It showed a clear separation between planktonic and surface associated communities (Fig. 3). In  
114 addition, a separation of epiphytic bacterial and archaeal communities based on host species was  
115 determined. This separation was further supported by ANOSIM ( $R = 0.96, p < 0.001$ ). Seasonal  
116 changes of *C. nodosa* associated communities indicated a separation between Spring, Summer  
117 and Autumn/Winter samples (ANOSIM,  $R = 0.54, p < 0.01$ ). For *C. cylindracea* associated  
118 communities a separation between Summer and Autumn/Winter/Spring samples was observed  
119 that was not so strongly supported (ANOSIM,  $R = 0.32, p < 0.01$ ) (Fig. 3).

120 The taxonomic composition of both, macrophyte associated and seawater communities,  
121 was dominated by bacterial ( $99.1 \pm 2.1$  %) over archaeal sequences ( $0.9 \pm 2.1$  %) (Fig. 4).  
122 Higher relative abundances of chloroplast related sequences were only observed in surface  
123 associated communities, with higher values in Autumn/Winter ( $37.2 \pm 11.2$  %) in comparison to  
124 Spring/Summer ( $20.9 \pm 9.7$  %) (Fig. S3). Generally, at higher taxonomic ranks (phylum-class)  
125 epiphytic and seawater microbial communities were composed of similar bacterial taxa.

126 Seawater communities were mainly comprised of *Actinobacteriota*, *Bacteroidota*, *Cyanobacteria*,  
127 *Alphaproteobacteria*, *Gammaproteobacteria* and *Verrucomicrobiota*. Communities associated  
128 with *C. nodosa* consisted of same groups with the addition of *Planctomycetota* whose contribution  
129 was higher in summer 2018. In addition, communities from mixed and monospecific *C.*  
130 *cylindracea* were similar and characterized by same groups as seawater and *C. nodosa*  
131 communities with the addition of *Desulfobacterota* (Fig. 4). Larger differences between  
132 environments and host species could be observed at lower taxonomic ranks (Fig. 5 – 9).

133 *Cyanobacteria* related sequences were comprising, on average,  $5.5 \pm 4.4\%$  of total sequences  
134 (Fig. 5). Higher proportions were found for *C. nodosa* ( $16.4 \pm 5.3\%$ ) and *C. cylindracea* (mixed  
135 [ $(7.7 \pm 3.9\%)$ ] and monospecific [ $(7.8 \pm 2.4\%)$ ]) associated communities in autumn and for  
136 seawater communities in winter ( $8.8 \pm 7.5\%$ ). Large taxonomic differences between surface  
137 associated and seawater cyanobacterial communities were observed. Seawater communities  
138 were mainly comprised of *Cyanobium* and *Synechococcus*, while surface associated communities  
139 were consisted of *Pleurocapsa* and sequences without known relatives within *Cyanobacteriia*  
140 (Fig. 5). In addition, seasonal changes in surface associated communities were observed with  
141 *Pleurocapsa* and no relative *Cyanobacteriia* comprising larger proportions in autumn and winter  
142 and *Acrophormium*, *Phormidesmis* and no relative *Nodosilineaceae* in spring and summer (Fig. 5).

143 Sequences classified as *Bacteroidota* were comprising, on average,  $19.2 \pm 5.5\%$  of all  
144 sequences (Fig. 6). Similarly to *Cyanobacteria*, large differences in the taxonomic composition  
145 between seawater and surface associated communities were found (Fig. 6). The seawater  
146 community was characterized by the NS4 and NS5 marine groups, uncultured *Cryomorphaceae*,  
147 uncultured *Flavobacteriaceae*, NS11-12 marine group, *Balneola*, uncultured *Balneolaceae* and  
148 *Formosa*. In contrast, in surface associated communities *Lewinella*, *Portibacter*, *Rubidimonas*, no  
149 relative *Saprospiraceae*, uncultured *Saprospiraceae*, no relative *Flavobacteriaceae* and uncultured  
150 *Rhodothermaceae* were found. Some groups showed slight seasonal changes such as no relative  
151 *Flavobacteriaceae* that were more pronounced from November 2017 until June 2018. In contrast,

152 uncultured *Rhodothermaceae* showed higher proportions from June 2018 until the end of the study  
153 period. Surface associated *Bacteroidota* communities were very diverse as could be observed in  
154 the high proportion of taxa that grouped as other *Bacteroidota* (Fig. 6).

155 On average, *Alphaproteobacteria* were in comparison to other high rank taxa the largest  
156 taxonomic group, comprising  $29.2 \pm 12.0$  % of all sequences (Fig. 7). In accordance to previous  
157 taxa, high differences between seawater and surface associated communities were observed.  
158 Picoplankton communities were composed mainly of the SAR11 clade, AEGEAN-169 marine  
159 group, SAR116 clade, no relative *Rhodobacteraceae*, HIMB11 and OCS116 clade, while surface  
160 associated communities were composed in high proportion of no relative *Rhodobacteraceae* and to  
161 a lesser degree of *Pseudoahrensia*, no relative *Alphaproteobacteria*, no relative *Hyphomonadaceae*  
162 and *Amylibacter*. Representatives of no relative *Rhodobacteraceae* were comprising on average  
163  $40.6 \pm 23.2$  % of all alphaproteobacterial sequences from the epiphytic community (Fig. 7). In  
164 addition, *Amylibacter* was detected mainly in *C. nodosa* from November 2017 until March 2018.

165 Sequences related to *Gammaproteobacteria* were comprising, on average,  $18.6 \pm 3.9$  %  
166 of all sequences (Fig. 8). Similarly to previous taxa, large taxonomic differences between  
167 seawater and surface associated communities were found. Seawater communities were mainly  
168 comprised of the OM60 (NOR5) clade, *Litoricola*, *Acinetobacter* and the SAR86 clade,  
169 while epiphytic communities were mainly composed of no relative *Gammaproteobacteria* and  
170 *Granulosicoccus*. Beside these two groups specific to all three epiphytic communities, *C. nodosa*  
171 was characterized by *Arenicella*, no relative *Burkholderiales* and *Methylotenera*, while *Thioploca*,  
172 no relative *Cellvibrionaceae* and *Reinekea* were more specific to both mixed and monospecific  
173 *C. cylindracea*. In addition, *Arenicella* was more pronounced in November and December 2017,  
174 while no relative *Burkholderiales* and *Methylotenera* were more characteristic for the period from  
175 March until May 2018. For the *C. cylindracea* specific taxa no relative *Cellvibrionaceae* and  
176 *Reinekea* showed some seasonality and were characteristic for samples originating from June to  
177 October 2018. In addition, similarly to *Bacteroidota*, a large proportion of the surface associated

<sup>178</sup> community was grouped as other *Gammaproteobacteria* indicating high diversity within this  
<sup>179</sup> group (Fig. 8).

<sup>180</sup> In contrast to previously described high rank taxa, *Desulfobacterota* were specific to *C.*  
<sup>181</sup> *cylindracea*. On average they comprised  $11.2 \pm 13.3$  % of all sequences. Seawater and *C.*  
<sup>182</sup> *nodosa* communities consisted of only  $0.1 \pm 0.08$  % and  $1.0 \pm 0.7$  % *Desulfobacterota* sequences,  
<sup>183</sup> respectively. In the mixed and monospecific *C. cylindracea* communities their proportion was  $25.7$   
<sup>184</sup>  $\pm 11.2$  % and  $24.0 \pm 4.3$  %, respectively (Fig. 9). The community consisted mainly of no relative  
<sup>185</sup> *Desulfobacteraceae*, *Desulfatitalea*, no relative *Desulfobulbaceae*, *Desulfobulbus*, no relative  
<sup>186</sup> *Desulfocapsaceae*, *Desulfopila*, *Desulforhopalus*, *Desulfotalea*, SEEP-SRB4 and uncultured  
<sup>187</sup> *Desulfocapsaceae* (Fig. 9).

188 **Discussion**

189 Surfaces of marine macrophytes harbor biofilms consisting of diverse microbial taxa (Egan  
190 *et al.*, 2013; Tarquinio *et al.*, 2019). No standard protocol has been developed to study these  
191 macrophyte associated microbes (Ugarelli *et al.*, 2019). Different procedures for removal of  
192 microbial cells from host surfaces were described, such as host tissue shaking (Nõges *et al.*, 2010),  
193 scraping (Uku *et al.*, 2007) and ultrasonication (Cai *et al.*, 2014). All these methods showed  
194 different removal efficiencies but none was enabling a complete removal of attached microbial  
195 cells. In the present study, we applied an earlier developed removal protocol (Korlević *et al.*,  
196 2020, submitted), based on a previous idea of direct cellular lysis (Burke *et al.*, 2009), to ensure an  
197 almost complete cell detachment. The application of a direct lysis procedure coupled with a high  
198 frequency sampling protocol and Illumina high resolution amplicon sequencing has enabled us to  
199 make a detailed description of bacterial and archaeal communities associated with the surfaces of  
200 two marine macrophytes, *C. nodosa* and *C. cylindracea*.

201 In the present study, highest richness values were observed for *C. cylindracea* (mixed and  
202 monospecific), middle for *C. nodosa* and lowest for seawater derived communities. Higher values  
203 for seagrass associated communities in comparison to seawater were described earlier and could  
204 be attributed to a larger set of inhabitable microniches existing on macrophyte surfaces (Ugarelli  
205 *et al.*, 2019). In addition, highest values observed for *C. cylindracea* are partly due to its contact  
206 with the sediment. *C. cylindracea* stolon is attached to the sediment surface with rhizoids, so  
207 the stolon and rhizoids are in a direct contact with the sediment. In addition, seasonal richness  
208 differences observed for surface attached communities showed slightly higher values in spring  
209 and summer. This pattern could be explained by a higher macrophyte growth in these seasons  
210 (M. Najdek, personal communication; Zavodnik *et al.*, 1998; Ruitton *et al.*, 2005). During active  
211 periods macrophytes exhibit a more dynamic chemical interaction with the surface community  
212 probably causing an increase in the number of inhabitable microniches (Borges and Champenois,  
213 2015; Rickert *et al.*, 2016).

214 Since the colonization of macrophyte surfaces is performed from a pool of prokaryotic cells  
215 from the ambient seawater, it was interesting to see to which extent these two communities differ.  
216 We observed a strong differentiation between the surface attached and seawater communities at  
217 the level of OTUs that is in agreement with most published studies (Burke and Thomas *et al.*,  
218 2011; Michelou *et al.*, 2013; Roth-Schulze *et al.*, 2016; Crump *et al.*, 2018; Ugarelli *et al.*, 2019).  
219 These data indicate that marine macrophytes are selecting, from a pool of seawater microbial taxa,  
220 the one that can colonize and proliferate on their surfaces (Salaün *et al.*, 2012; Michelou *et al.*,  
221 2013). In contrast to these findings Fahimipour *et al.* (2017) found, in a global study of *Zostera*  
222 *marina*, similarities between leaves and seawater samples. Discrepancies between our data and this  
223 study could be explained by differences in studied seagrass species, methodological variations or  
224 biogeographic trends as Fahimipour *et al.* (2017) were analyzing samples from different locations  
225 throughout the northern hemisphere. It is possible that ambient seawater and leaves communities  
226 from the same location are differing but are still more similar to each other when compared to  
227 other sampling locations. Indeed, it was found that prokaryotic communities vary substantially  
228 between different sampling sites (Bengtsson *et al.*, 2017). When the taxonomic composition at  
229 high ranks was analyzed no such strong differentiation was noticed. Phyla and classes such as:  
230 *Actinobacteriota*, *Bacteroidota*, *Cyanobacteria*, *Alphaproteobacteria*, *Gammaproteobacteria* and  
231 *Verrucomicrobiota* were described that is in agreement with previously reported data (Burke and  
232 Thomas *et al.*, 2011; Egan *et al.*, 2013; Michelou *et al.*, 2013). In contrast, when low taxonomic  
233 ranks were analyzed (i.g. family and genus) a strong differentiation was observed. A similar  
234 differentiation at lower taxonomic ranks was described for other species of macrophytes (Egan *et*  
235 *al.*, 2013; Michelou *et al.*, 2013; Ugarelli *et al.*, 2019).

236 Beside differences between seawater and surface associated communities, there were  
237 discussions if the prokaryotic epiphytic community is host-specific or there are generalists taxa  
238 characteristic to all or many macrophytes (Egan *et al.*, 2013). Similarly to previously described  
239 differences between seawater and surface attached communities, at high taxonomic ranks no  
240 strong differentiation between communities associated with different host was observed. The only

241 high rank phylum that was differing between *C. nodosa* and *C. cylindracea* was *Desulfobacterota*,  
242 whose sequences were more abundant in the *C. cylindracea* associated community. As already  
243 mentioned, the rhizoids and part of the stolon are in contact with the sediment, so *Desulfobacterota*  
244 are probably a part of the epiphytic community that was in contact with the sediment. Similar  
245 high rank taxa found in this study were described to be specific for other species of macrophytes  
246 (Burke and Thomas *et al.*, 2011; Lachnit *et al.*, 2011; Bengtsson *et al.*, 2017). In contrast to  
247 high taxonomic ranks, a substantial differentiation between host specific communities was found,  
248 which supports the host-specific hypothesis. Similar host-specificity was observed for different  
249 species of macroalgae and seagrasses (Lachnit *et al.*, 2011; Roth-Schulze *et al.*, 2016; Ugarelli *et*  
250 *al.*, 2019; Morrissey *et al.*, 2019). Taken together, at high taxonomic ranks a core set of taxa could  
251 be described that is characteristic for all or many macrophytes, while at low taxonomic ranks a  
252 community specific to host species could be identified (Egan *et al.*, 2013).

253 Seasonal richness changes in the epiphytic community were substantial as could be observed  
254 in the proportion of OTUs that could be found at every sampling time ( $\leq 1.0\%$ ). Interestingly,  
255 these OTUs were accounting for a high proportion of sequences ( $\leq 52.5\%$ ). A very similar  
256 proportion of persistent OTUs and their sequence contribution was reported in high frequency  
257 studies describing seasonal picoplankton changes (Gilbert *et al.*, 2009, 2012). In comparison to  
258 the seawater community, a lower degree of seasonal shifts was observed for the surface associated  
259 communities. It seems, microniches on the surfaces of macrophytes are providing more stable  
260 conditions in comparison to the seawater. At the level of OTUs seasonal changes of *C. nodosa* and  
261 *C. cylindracea* associated communities were identified that could be linked to the growth cycle of  
262 the seagrass and macroalgae (M. Najdek, personal communication). *C. nodosa* was characterized  
263 by a Spring community during maximum seagrass proliferation, a Summer community during a  
264 biomass maximum and a Autumn/Winter community during a biomass senescence. In contrast,  
265 *C. cylindracea* started to proliferate in late Spring and was characterized only by a Summer  
266 community during maximal biomass increase and by a Autumn/Winter/Spring community when  
267 the biomass was at the peak and the settlement started to subsequently decay. Similar seasonal

268 changes in the epiphytic community was also described for other macroalgae (Tujula *et al.*,  
269 2010; Lachnit *et al.*, 2011). Higher temporal stability of *C. cylindracea* surface communities  
270 in comparison to *C. nodosa* were also observed in the higher proportion of shared communities  
271 between two consecutive sampling points.

272 Analysis of seasonal chloroplast sequence abundances showed higher values in Autumn/Winter  
273 in comparison to Spring/Summer. This pattern is not surprising as seagrasses are known to harbor  
274 more algal epiphytes during Autumn/Winter (Reyes and Sansón, 2001). Furthermore, we used  
275 an adapted DNA isolation protocol that is known to partially coextract DNA from planktonic  
276 eukaryotes (Korlević *et al.*, 2015). Strong seasonal fluctuations of high rank epiphytic taxa  
277 were not observed, with the exception of *Cyanobacteria*. Cyanobacterial sequences were more  
278 pronounced in November and December in comparison to Spring and Summer. Interestingly,  
279 in these high proportion months the majority of cyanobacterial sequences were classified as  
280 *Pleurocapsa*, a group known to colonized different living and nonliving surfaces (Burns *et al.*,  
281 2004; Longford *et al.*, 2007; Mobberley *et al.*, 2012; Reisser *et al.*, 2014). It is possible that during  
282 periods of low metabolic activity there is a reduced interaction and selection of the epiphytic  
283 community by the seagrass, causing leaves to become a suitable surface for nonspecific colonizers  
284 (Zavodnik *et al.*, 1998). *Pleurocapsa* was replaced in Spring and Summer by *Acrophormium*,  
285 *Phormidesmis* and no relative *Nodosilineaceae*. A study of coastal microbial mats found also  
286 higher proportion of *Nodosilineaceae* sequences in Summer, while *Phormidesmis* sequences  
287 were at their peak in Autumn (Cardoso *et al.*, 2019). Other high rank taxa did not show strong  
288 successional patterns. In every analyzed group, with the exception of *Desulfobacterota*, taxa  
289 present throughout the year in similar proportions and season specific taxa could be identified.  
290 Within *Bacteroidota* different groups withing the family *Sapspiraceae* (i.g. *Lewinella*,  
291 *Portibacter* and *Rubidimonas*) were detected through the year. Members of this family are  
292 often found in association with macrophytes and it is suggested that they are involved in the  
293 hydrolysis and utilization of complex carbon sources (Burke and Thomas *et al.*, 2011; McIlroy  
294 and Nielsen, 2014; Crump *et al.*, 2018). On the other hand, families *Flavobacteriaceae* and

295 *Rhodothermaceae* showed seasonal patterns, with *Flavobacteriaceae* being more pronounced  
296 from November to June and *Rhodothermaceae* from June to October. Within *Alphaproteobacteria*  
297 the family *Rhodobacteraceae* was comprising the majority of sequences throughout the year. This  
298 metabolically versatile family is often associated with macrophyte surfaces and usually is one  
299 of the most abundant groups (Burke and Thomas *et al.*, 2011; Michelou *et al.*, 2013; Pujalte *et*  
300 *al.*, 2014). In addition, *Hyphomonadaceae* were found in all samples. Interestingly, some of the  
301 species within this group contain stalks on their cells which can be used to attach to the macrophyte  
302 surface (Weidner *et al.*, 2000; Abraham and Rohde, 2014). Within the *Gammaproteobacteria*,  
303 sequences without known representatives were the most pronounced group present throughout the  
304 year. In addition, *Granulosicoccus* was also found in almost all samples. *Gammaproteobacteria*  
305 are often a major constituent of macrophyte epiphytic communities (Burke and Thomas *et al.*,  
306 2011; Michelou *et al.*, 2013; Crump *et al.*, 2018). Beside these two groups other less pronounced  
307 taxa showed seasonal and host-specific patterns. For example, *C. cylindracea* was characterized  
308 by *Thioploca*, a known sulfur sediment bacteria and *Cellvibrionaceae*, a family whose cultured  
309 members are known polysaccharide degraders (Jørgensen and Gallardo, 1999; Xie *et al.*, 2017).  
310 *Desulfobacterota* were found only associated with *C. cylindracea* and no group within this phylum  
311 showed seasonal patterns. The presence of this phylum only on *C. cylindracea* is to be expected  
312 as part of the epiphytic community is directly in contact with the sediment. The *Desulfobacterota*  
313 community was dominated by *Desulfatitalea* and no relative *Desulfocapsaceae*, known sulfate  
314 sediment groups (Kuever, 2014; Higashioka *et al.*, 2015).

315 In temperate zones marine macrophytes are exhibiting growth cycles, so it is not surprising  
316 that the associated epiphytic microbial community is undergoing partial seasonal changes. In  
317 the present study, we could, in every analyzed high rank taxa, identify phylogenetic groups  
318 that were present throughout the year and that were comprising most of the sequences and  
319 lower proportion taxa showing seasonal patterns connected to the macrophyte growth cycle.  
320 Studies focusing on functional comparisons between communities associated with different  
321 hosts showed that the majority of functions could be found in every community, indicating

322 functional redundancy (Roth-Schulze *et al.*, 2016). This difference between taxonomic and  
323 functional discrepancy was explained by the lottery hypothesis that hypothesizes an initial random  
324 colonization step performed from a set of functionally equivalent taxonomic groups (Burke and  
325 Peter Steinberg *et al.*, 2011; Roth-Schulze *et al.*, 2016). It is possible that functional redundancy is  
326 a characteristic of high abundance taxa detected to be present throughout the year, while seasonal  
327 and/or host-specific functions are an attribute of taxa displaying successional patterns. Further  
328 studies connecting taxonomy with functional properties will be required to elucidate the degree of  
329 functional redundancy or specificity in epiphytic microbial communities.

330 **Experimental procedures**

331 **Sampling**

332 Sampling was performed in the Bay of Funtana, northern Adriatic Sea (45°10'39" N,  
333 13°35'42" E). Leaves and thalli were sampled in a meadow of *Cymodocea nodosa* invaded by the  
334 invasive *Caulerpa cylindracea* (mixed settlement) and in a monospecific settlement of *Caulerpa*  
335 *cylindracea* located in the proximity of the meadow at approximately monthly intervals from  
336 December 2017 to October 2018 (Table S1). Leaves and thalli were collected by diving and  
337 transported to the laboratory in containers placed on ice and filled with site seawater. Upon arrival  
338 to the laboratory, *C. nodosa* leaves were cut into sections of 1 – 2 cm, while *C. cylindracea* thalli  
339 were cut into 5 – 8 cm long sections. Leaves and thalli were washed three times with sterile  
340 artificial seawater (ASW) to remove loosely attached microbial cells. Ambient seawater was  
341 collected in 10 l containers by diving and transported to the laboratory where the whole container  
342 volume was filtered through a 20 µm net. The filtrate was further sequentially filtered through 3  
343 µm and 0.2 µm polycarbonate membrane filters (Whatman, United Kingdom) using a peristaltic  
344 pump. Filters were briefly dried at room temperature and stored at –80 °C. Seawater samples  
345 were also collected approximately monthly from July 2017 to October 2018.

346 **DNA isolation**

347 DNA from surfaces of *C. nodosa* and *C. cylindracea* was isolated using a previously modified  
348 and adapted protocol that allows for a selective epiphytic DNA isolation (Massana *et al.*, 1997;  
349 Korlević *et al.*, 2020, submitted). Briefly, leaves and thalli are incubated in a lysis buffer and  
350 treated with lysozyme and proteinase K. Following the incubations, the mixture containing  
351 lysed epiphytic cells is separated from leaves and thalli and extracted using a phenol-chloroform  
352 procedure. Finally, the extracted DNA is precipitated using isopropanol. DNA from seawater

353 picoplankton was isolated from 0.2  $\mu$ m polycarbonate filters according to Massana *et al.* (1997)  
354 with a slight modification. Following the phenol-chloroform extraction steps 1/10 of chilled 3  
355 M sodium acetate (pH 5.2) was added. DNA was precipitated by adding 1 volume of chilled  
356 isopropanol, incubating the mixtures overnight at -20 °C and centrifuging at 20,000  $\times$  g and 4 °C  
357 for 21 min. The pellet was washed twice with 500  $\mu$ l of chilled 70 % ethanol and centrifuged after  
358 each washing step at 20,000  $\times$  g and 4 °C for 5 min. Dried pellets were resuspended in 50 – 100  
359  $\mu$ l of deionized water.

360 **Illumina 16S rRNA sequencing**

361 Illumina MiSeq sequencing of the V4 16S rRNA region was performed as described  
362 previously (Korlević *et al.*, 2020, submitted). The V4 region of the 16S rRNA gene was amplified  
363 using a two-step PCR procedure. In the first PCR the 515F (5'-GTGYCAGCMGCCGCGTAA-3')  
364 and 806R (5'-GGACTACNVGGGTWTCTAAT-3') primers from the Earth Microbiome Project  
365 (<http://press.igsb.anl.gov/earthmicrobiome/protocols-and-standards/16s/>) were used (Caporaso  
366 *et al.*, 2012; Apprill *et al.*, 2015; Parada *et al.*, 2016). These primers contained on their 5' end  
367 a tagged sequence. Purified PCR products were sent for Illumina MiSeq sequencing at IMGM  
368 Laboratories, Martinsried, Germany. Before sequencing at IMGM, the second PCR amplification  
369 of the two-step PCR procedure was performed using primers targeting the tagged region  
370 incorporated in the first PCR. In addition, these primers contained adapter and sample-specific  
371 index sequences. Beside samples, a positive and negative control for each sequencing batch was  
372 sequenced. Negative control was comprised of PCR reactions without DNA template, while for  
373 a positive control a mock community composed of evenly mixed DNA material originating from  
374 20 bacterial strains (ATCC MSA-1002, ATCC, USA) was used. Sequences obtained in this study  
375 have been deposited in the European Nucleotide Archive (ENA) at EMBL-EBI under accession  
376 number PRJEB37267.

377 **Sequence analysis**

378       Obtained sequences were analyzed on the computer cluster Isabella (University Computing  
379       Center, University of Zagreb) using mothur (version 1.43.0) (Schloss *et al.*, 2009) according  
380       to the MiSeq Standard Operating Procedure (MiSeq SOP; [https://mothur.org/wiki/MiSeq\\_SOP](https://mothur.org/wiki/MiSeq_SOP))  
381       (Kozich *et al.*, 2013) and recommendations given from the Riffomonas project to enhance data  
382       reproducibility (<http://www.riffomonas.org/>). For alignment and classification of sequences the  
383       SILVA SSU Ref NR 99 database (release 138; <http://www.arb-silva.de>) was used (Quast *et al.*,  
384       2013; Yilmaz *et al.*, 2014). Pipeline data processing and visualization was done using R (version  
385       3.6.0) (R Core Team, 2019), packages vegan (version 2.5-6) (Oksanen *et al.*, 2019), and tidyverse  
386       (version 1.3.0) (Wickham *et al.*, 2019) and multiple other packages (Xie, 2014, 2015, 2020;  
387       Neuwirth, 2014; Xie *et al.*, 2018; Y. Xie, 2019b, 2019a; Allaire *et al.*, 2019; Zhu, 2019). The  
388       detailed analysis procedure including the R Markdown file for this paper are available as a GitHub  
389       repository ([https://github.com/mkorlevic/Korlevic\\_EpiphyticDynamics\\_EnvironMicrobiol\\_2020](https://github.com/mkorlevic/Korlevic_EpiphyticDynamics_EnvironMicrobiol_2020)).  
390       Based on the ATCC MSA-1002 mock community included in the analysis an average sequencing  
391       error rate of 0.01 % was determined, which is in line with previously reported values for  
392       next-generation sequencing data (Kozich *et al.*, 2013; Schloss *et al.*, 2016). In addition, the  
393       negative controls processed together with the samples yielded on average only 2 sequences after  
394       sequence quality curation.

395 **Acknowledgments**

396       This work was founded by the Croatian Science Foundation through the MICRO-SEAGRASS  
397       project (IP-2016-06-7118). We would like to thank Margareta Buterer for technical support, Paolo  
398       Paliaga for help during sampling and the University Computing Center of the University of Zagreb  
399       for access to the cluster Isabella.

400 **References**

- 401 Abraham, W.R. and Rohde, M. (2014) The family *Hyphomonadaceae*. In *The Prokaryotes: Alphaproteobacteria and Betaproteobacteria*. Rosenberg, E., DeLong, E.F., Lory, S., Stackebrandt, E., and Thompson, F. (eds). Berlin, Heidelberg: Springer-Verlag, pp. 283–299.
- 404 Allaire, J.J., Xie, Y., McPherson, J., Luraschi, J., Ushey, K., Atkins, A., et al. (2019) Rmarkdown: Dynamic documents for R.
- 406 Apprill, A., McNally, S., Parsons, R., and Weber, L. (2015) Minor revision to V4 region SSU rRNA 806R gene primer greatly increases detection of SAR11 bacterioplankton. *Aquat Microb Ecol* **75**: 129–137.
- 409 Armstrong, E., Rogerson, A., and Leftley, J. (2000) The abundance of heterotrophic protists associated with intertidal seaweeds. *Estuar Coast Shelf Sci* **50**: 415–424.
- 411 Bengtsson, M.M., Bühler, A., Brauer, A., Dahlke, S., Schubert, H., and Blindow, I. (2017) 412 Eelgrass leaf surface microbiomes are locally variable and highly correlated with epibiotic 413 eukaryotes. *Front Microbiol* **8**: 1312.
- 414 Bengtsson, M., Sjøtun, K., and Øvreås, L. (2010) Seasonal dynamics of bacterial biofilms on 415 the kelp *Laminaria hyperborea*. *Aquat Microb Ecol* **60**: 71–83.
- 416 Borges, A.V. and Champenois, W. (2015) Seasonal and spatial variability of dimethylsulfoniopropionate 417 (DMSP) in the Mediterranean seagrass *Posidonia oceanica*. *Aquat Bot* **125**: 72–79.
- 418 Burke, C., Kjelleberg, S., and Thomas, T. (2009) Selective extraction of bacterial DNA from 419 the surfaces of macroalgae. *Appl Environ Microbiol* **75**: 252–256.
- 420 Burke, C., Steinberg, P., Rusch, D., Kjelleberg, S., and Thomas, T. (2011) Bacterial 421 community assembly based on functional genes rather than species. *Proc Natl Acad Sci U S A*

422 108: 14288–14293.

423 Burke, C., Thomas, T., Lewis, M., Steinberg, P., and Kjelleberg, S. (2011) Composition,  
424 uniqueness and variability of the epiphytic bacterial community of the green alga *Ulva australis*.  
425 *ISME J* **5**: 590–600.

426 Burns, B.P., Goh, F., Allen, M., and Neilan, B.A. (2004) Microbial diversity of extant  
427 stromatolites in the hypersaline marine environment of Shark Bay, Australia. *Environ Microbiol*  
428 **6**: 1096–1101.

429 Cai, X., Gao, G., Yang, J., Tang, X., Dai, J., Chen, D., and Song, Y. (2014) An ultrasonic  
430 method for separation of epiphytic microbes from freshwater submerged macrophytes. *J Basic*  
431 *Microbiol* **54**: 758–761.

432 Caporaso, J.G., Lauber, C.L., Walters, W.A., Berg-Lyons, D., Huntley, J., Fierer, N., et al.  
433 (2012) Ultra-high-throughput microbial community analysis on the Illumina HiSeq and MiSeq  
434 platforms. *ISME J* **6**: 1621–1624.

435 Cardoso, D.C., Cretoiu, M.S., Stal, L.J., and Bolhuis, H. (2019) Seasonal development of a  
436 coastal microbial mat. *Sci Rep* **9**: 9035.

437 Crump, B.C. and Koch, E.W. (2008) Attached bacterial populations shared by four species of  
438 aquatic angiosperms. *Appl Environ Microbiol* **74**: 5948–5957.

439 Crump, B.C., Wojahn, J.M., Tomas, F., and Mueller, R.S. (2018) Metatranscriptomics and  
440 amplicon sequencing reveal mutualisms in seagrass microbiomes. *Front Microbiol* **9**: 388.

441 Egan, S., Harder, T., Burke, C., Steinberg, P., Kjelleberg, S., and Thomas, T. (2013) The  
442 seaweed holobiont: Understanding seaweed-bacteria interactions. *FEMS Microbiol Rev* **37**:  
443 462–476.

444 Fahimipour, A.K., Kardish, M.R., Lang, J.M., Green, J.L., Eisen, J.A., and Stachowicz, J.J.

- 445 (2017) Global-scale structure of the eelgrass microbiome. *Appl Environ Microbiol* **83**: e03391–16.
- 446        Gilbert, J.A., Field, D., Swift, P., Newbold, L., Oliver, A., Smyth, T., et al. (2009) The  
447        seasonal structure of microbial communities in the Western English Channel. *Environ Microbiol*  
448        **11**: 3132–3139.
- 449        Gilbert, J.A., Steele, J.A., Caporaso, J.G., Steinbrück, L., Reeder, J., Temperton, B., et al.  
450        (2012) Defining seasonal marine microbial community dynamics. *ISME J* **6**: 298–308.
- 451        Higashioka, Y., Kojima, H., Watanabe, T., and Fukui, M. (2015) Draft genome sequence of  
452        *Desulfatitalea tepidiphila* S28bF<sup>T</sup>. *Genome Announc* **3**: e01326–15.
- 453        Hollants, J., Leliaert, F., De Clerck, O., and Willems, A. (2013) What we can learn from  
454        sushi: A review on seaweed-bacterial associations. *FEMS Microbiol Ecol* **83**:
- 455        Jost, L. (2006) Entropy and diversity. *Oikos* **113**: 363–375.
- 456        Jørgensen, B.B. and Gallardo, V.A. (1999) *Thioploca* spp.: filamentous sulfur bacteria with  
457        nitrate vacuoles. *FEMS Microbiol Ecol* **28**: 301–313.
- 458        Korlević, M., Markovski, M., Zhao, Z., Herndl, G.J., and Najdek, M. (2020) Selective DNA  
459        and protein isolation from marine macrophyte surfaces.
- 460        Korlević, M., Pop Ristova, P., Garić, R., Amann, R., and Orlić, S. (2015) Bacterial diversity  
461        in the South Adriatic Sea during a strong, deep winter convection year. *Appl Environ Microbiol*  
462        **81**: 1715–1726.
- 463        Kozich, J.J., Westcott, S.L., Baxter, N.T., Highlander, S.K., and Schloss, P.D. (2013)  
464        Development of a dual-index sequencing strategy and curation pipeline for analyzing amplicon  
465        sequence data on the MiSeq Illumina sequencing platform. *Appl Environ Microbiol* **79**:  
466        5112–5120.

467 Kuever, J. (2014) The family *Desulfobulbaceae*. In *The Prokaryotes: Deltaproteobacteria*  
468 and *Epsilonproteobacteria*. Rosenberg, E., DeLong, E.F., Lory, S., Stackebrandt, E., and  
469 Thompson, F. (eds). Berlin, Heidelberg: Springer-Verlag, pp. 75–86.

470 Lachnit, T., Blümel, M., Imhoff, J.F., and Wahl, M. (2009) Specific epibacterial communities  
471 on macroalgae: Phylogeny matters more than habitat. *Aquat Biol* **5**: 181–186.

472 Lachnit, T., Meske, D., Wahl, M., Harder, T., and Schmitz, R. (2011) Epibacterial community  
473 patterns on marine macroalgae are host-specific but temporally variable. *Environ Microbiol* **13**:  
474 655–665.

475 Longford, S., Tujula, N., Crocetti, G., Holmes, A., Holmström, C., Kjelleberg, S., et al. (2007)  
476 Comparisons of diversity of bacterial communities associated with three sessile marine eukaryotes.  
477 *Aquat Microb Ecol* **48**: 217–229.

478 Margulis, L. (1991) Symbiogenesis and symbioticism. In *Symbiosis as a Source of*  
479 *Evolutionary Innovation: Speciation and Morphogenesis*. Margulis, L. and Fester, R. (eds).  
480 Cambridge, Massachusetts: The MIT Press, pp. 1–14.

481 Massana, R., Murray, A.E., Preston, C.M., and DeLong, E.F. (1997) Vertical distribution and  
482 phylogenetic characterization of marine planktonic *Archaea* in the Santa Barbara Channel. *Appl*  
483 *Environ Microbiol* **63**: 50–56.

484 McIlroy, S.J. and Nielsen, P.H. (2014) The family *Saprospiraceae*. In *The Prokaryotes: Other*  
485 *Major Lineages of Bacteria and the Archaea*. Rosenberg, E., DeLong, E.F., Lory, S., Stackebrandt,  
486 E., and Thompson, F. (eds). Berlin, Heidelberg: Springer-Verlag, pp. 863–889.

487 Michelou, V.K., Caporaso, J.G., Knight, R., and Palumbi, S.R. (2013) The ecology of  
488 microbial communities associated with *Macrocystis pyrifera*. *PloS One* **8**: e67480.

489 Miranda, L.N., Hutchison, K., Grossman, A.R., and Brawley, S.H. (2013) Diversity and

490 abundance of the bacterial community of the red macroalga *Porphyra umbilicalis*: Did bacterial  
491 farmers produce macroalgae? *PLoS One* **8**: e58269.

492 Mobberley, J.M., Ortega, M.C., and Foster, J.S. (2012) Comparative microbial diversity  
493 analyses of modern marine thrombolitic mats by barcoded pyrosequencing. *Environ Microbiol* **14**:  
494 82–100.

495 Morrissey, K.L., Çavas, L., Willems, A., and De Clerck, O. (2019) Disentangling the influence  
496 of environment, host specificity and thallus differentiation on bacterial communities in siphonous  
497 green seaweeds. *Front Microbiol* **10**: 717.

498 Neuwirth, E. (2014) RColorBrewer: ColorBrewer palettes.

499 Nõges, T., Luup, H., and Feldmann, T. (2010) Primary production of aquatic macrophytes  
500 and their epiphytes in two shallow lakes (Peipsi and Võrtsjärv) in Estonia. *Aquat Ecol* **44**: 83–92.

501 Oksanen, J., Blanchet, F.G., Friendly, M., Kindt, R., Legendre, P., McGlinn, D., et al. (2019)  
502 Vegan: Community ecology package.

503 Parada, A.E., Needham, D.M., and Fuhrman, J.A. (2016) Every base matters: Assessing  
504 small subunit rRNA primers for marine microbiomes with mock communities, time series and  
505 global field samples. *Environ Microbiol* **18**: 1403–1414.

506 Pujalte, M.J., Lucena, T., Ruvira, M.A., Arahal, D.R., and Macián, M.C. (2014) The  
507 family *Rhodobacteraceae*. In *The Prokaryotes: Alphaproteobacteria and Betaproteobacteria*.  
508 Rosenberg, E., DeLong, E.F., Lory, S., Stackebrandt, E., and Thompson, F. (eds). Berlin,  
509 Heidelberg: Springer-Verlag, pp. 439–512.

510 Quast, C., Pruesse, E., Yilmaz, P., Gerken, J., Schweer, T., Yarza, P., et al. (2013) The SILVA  
511 ribosomal RNA gene database project: Improved data processing and web-based tools. *Nucleic  
512 Acids Res* **41**: D590–D596.

- 513 R Core Team (2019) A language and environment for statistical computing, Vienna, Austria:
- 514 R Foundation for Statistical Computing.
- 515 Reisser, J., Shaw, J., Hallegraeff, G., Proietti, M., Barnes, D.K.A., Thums, M., et al. (2014)
- 516 Millimeter-sized marine plastics: A new pelagic habitat for microorganisms and invertebrates.
- 517 *PloS One* **9**: e100289.
- 518 Reyes, J. and Sansón, M. (2001) Biomass and production of the epiphytes on the leaves of
- 519 *Cymodocea nodosa* in the Canary Islands. *Bot Mar* **44**: 307–313.
- 520 Rickert, E., Wahl, M., Link, H., Richter, H., and Pohnert, G. (2016) Seasonal variations in
- 521 surface metabolite composition of *Fucus vesiculosus* and *Fucus serratus* from the Baltic Sea. *PloS*
- 522 *One* **11**: e0168196.
- 523 Roth-Schulze, A.J., Zozaya-Valdés, E., Steinberg, P.D., and Thomas, T. (2016) Partitioning
- 524 of functional and taxonomic diversity in surface-associated microbial communities. *Environ*
- 525 *Microbiol* **18**: 4391–4402.
- 526 Ruitton, S., Verlaque, M., and Boudouresque, C.F. (2005) Seasonal changes of the introduced
- 527 *Caulerpa racemosa* var. *cylindracea* (Caulerpales, Chlorophyta) at the northwest limit of its
- 528 Mediterranean range. *Aquat Bot* **82**: 55–70.
- 529 Salaün, S., La Barre, S., Santos-Goncalvez, M.D., Potin, P., Haras, D., and Bazire, A. (2012)
- 530 Influence of exudates of the kelp *Laminaria digitata* on biofilm formation of associated and
- 531 exogenous bacterial epiphytes. *Microb Ecol* **64**: 359–369.
- 532 Schloss, P.D., Jenior, M.L., Koumpouras, C.C., Westcott, S.L., and Highlander, S.K. (2016)
- 533 Sequencing 16S rRNA gene fragments using the PacBio SMRT DNA sequencing system. *PeerJ*
- 534 **4**: e1869.
- 535 Schloss, P.D., Westcott, S.L., Ryabin, T., Hall, J.R., Hartmann, M., Hollister, E.B., et al.

536 (2009) Introducing mothur: Open-source, platform-independent, community-supported software  
537 for describing and comparing microbial communities. *Appl Environ Microbiol* **75**: 7537–7541.

538 Tarquinio, F., Hyndes, G.A., Laverock, B., Koenders, A., and Säwström, C. (2019) The  
539 seagrass holobiont: Understanding seagrass-bacteria interactions and their role in seagrass  
540 ecosystem functioning. *FEMS Microbiol Lett* **366**: fnz057.

541 Tujula, N.A., Crocetti, G.R., Burke, C., Thomas, T., Holmström, C., and Kjelleberg, S. (2010)  
542 Variability and abundance of the epiphytic bacterial community associated with a green marine  
543 *Ulvacean* alga. *ISME J* **4**: 301–311.

544 Ugarelli, K., Laas, P., and Stingl, U. (2019) The microbial communities of leaves and roots  
545 associated with turtle grass (*Thalassia testudinum*) and manatee grass (*Syringodium filiforme*) are  
546 distinct from seawater and sediment communities, but are similar between species and sampling  
547 sites. *Microorganisms* **7**: 4.

548 Uku, J., Björk, M., Bergman, B., and Díez, B. (2007) Characterization and comparison of  
549 prokaryotic epiphytes associated with three East African seagrasses. *J Phycol* **43**: 768–779.

550 Weidner, S., Arnold, W., Stackebrandt, E., and Pühler, A. (2000) Phylogenetic analysis  
551 of bacterial communities associated with leaves of the seagrass *Halophila stipulacea* by a  
552 culture-independent small-subunit rRNA gene approach. *Microb Ecol* **39**: 22–31.

553 Wickham, H., Averick, M., Bryan, J., Chang, W., McGowan, L.D., François, R., et al. (2019)  
554 Welcome to the tidyverse. *J Open Source Softw* **4**: 1686.

555 Xie, Y. (2015) Dynamic Documents with R and knitr, 2nd ed. Boca Raton, Florida: Chapman  
556 and Hall/CRC.

557 Xie, Y. (2014) Knitr: A comprehensive tool for reproducible research in R. In *Implementing*  
558 *Reproducible Computational Research*. Stodden, V., Leisch, F., and Peng, R.D. (eds). New York:

- 559 Chapman and Hall/CRC, pp. 3–32.
- 560 Xie, Y. (2019a) Knitr: A general-purpose package for dynamic report generation in R.
- 561 Xie, Y. (2019b) TinyTeX: A lightweight, cross-platform, and easy-to-maintain LaTeX
- 562 distribution based on TeX Live. *TUGboat* **40**: 30–32.
- 563 Xie, Y. (2020) TinyTeX: Helper functions to install and maintain 'TeX Live', and compile
- 564 'LaTeX' documents.
- 565 Xie, Y., Allaire, J.J., and Grolemund, G. (2018) R Markdown: The Definitive Guide, 1st ed.
- 566 Boca Raton, Florida: Chapman and Hall/CRC.
- 567 Xie, Z., Lin, W., and Luo, J. (2017) Comparative phenotype and genome analysis of *Cellvibrio*
- 568 sp. PR1, a xylanolytic and agarolytic bacterium from the Pearl River. *BioMed Res Int* **2017**:
- 569 6304248.
- 570 Yilmaz, P., Parfrey, L.W., Yarza, P., Gerken, J., Pruesse, E., Quast, C., et al. (2014) The
- 571 SILVA and "All-Species Living Tree Project (LTP)" taxonomic frameworks. *Nucleic Acids Res*
- 572 **42**: D643–D648.
- 573 Zavodnik, N., Travizi, A., and de Rosa, S. (1998) Seasonal variations in the rate of
- 574 photosynthetic activity and chemical composition of the seagrass *Cymodocea nodosa* (Ucr.) Asch.
- 575 *Sci Mar* **62**: 301–309.
- 576 Zhu, H. (2019) KableExtra: Construct complex table with 'kable' and pipe syntax.

577 **Figure legends**

578 **Fig. 1.** Proportion of shared bacterial and archaeal OTUs (Jaccard's Similarity Coefficient)  
579 and shared bacterial and archaeal communities (Bray-Curtis Similarity Coefficient) between  
580 assemblages associated with the surfaces of macrophytes (*C. nodosa* [Mixed Settlement] and *C.*  
581 *cylindracea* [Mixed and Monospecific Settlement]) and communities in the ambient seawater.

582 **Fig. 2.** Proportion of shared bacterial and archaeal communities (Bray-Curtis Similarity  
583 Coefficient) and shared bacterial and archaeal OTUs (Jaccard's Similarity Coefficient) between  
584 consecutive sampling points and from the surfaces of macrophytes (*C. nodosa* [Mixed Settlement]  
585 and *C. cylindracea* [Mixed and Monospecific Settlement]) and in the ambient seawater.

586 **Fig. 3.** Principal Coordinates Analysis (PCoA) of Bray-Curtis distances based on OTU  
587 abundances of bacterial and archaeal communities from the surfaces of macrophytes (*C. nodosa*  
588 [Mixed Settlement] and *C. cylindracea* [Mixed and Monospecific Settlement]) and in the ambient  
589 seawater. Samples from the same environment or same season are labeled in different colors. The  
590 proportion of explained variation by each axis is shown on the corresponding axis in parentheses.

591 **Fig. 4.** Taxonomic classification and relative contribution of the most abundant (> 1 %) bacterial  
592 and archaeal sequences on the surfaces of macrophytes (*C. nodosa* [Mixed Settlement] and *C.*  
593 *cylindracea* [Mixed and Monospecific Settlement]) and in the ambient seawater. NR – No Relative

594 **Fig. 5.** Taxonomic classification and relative contribution of the most abundant (> 1 %)  
595 cyanobacterial sequences on the surfaces of macrophytes (*C. nodosa* [Mixed Settlement] and *C.*  
596 *cylindracea* [Mixed and Monospecific Settlement]) and in the ambient seawater. The proportion  
597 of cyanobacterial sequences in the total bacterial and archaeal community is given above the  
598 corresponding bar. NR – No Relative

599 **Fig. 6.** Taxonomic classification and relative contribution of the most abundant (> 2 %) sequences  
600 within the *Bacteroidota* on the surfaces of macrophytes (*C. nodosa* [Mixed Settlement] and *C.*

601 *cylindracea* [Mixed and Monospecific Settlement]) and in the ambient seawater. The proportion of  
602 sequences classified as *Bacteroidota* in the total bacterial and archaeal community is given above  
603 the corresponding bar. NR – No Relative

604 **Fig. 7.** Taxonomic classification and relative contribution of the most abundant (> 2 %)  
605 alphaproteobacterial sequences on the surfaces of macrophytes (*C. nodosa* [Mixed Settlement]  
606 and *C. cylindracea* [Mixed and Monospecific Settlement]) and in the ambient seawater. The  
607 proportion of alphaproteobacterial sequences in the total bacterial and archaeal community is  
608 given above the corresponding bar. NR – No Relative

609 **Fig. 8.** Taxonomic classification and relative contribution of the most abundant (> 2 %)  
610 gammaproteobacterial sequences on the surfaces of macrophytes (*C. nodosa* [Mixed Settlement]  
611 and *C. cylindracea* [Mixed and Monospecific Settlement]) and in the ambient seawater. The  
612 proportion of gammaproteobacterial sequences in the total bacterial and archaeal community is  
613 given above the corresponding bar. NR – No Relative

614 **Fig. 9.** Taxonomic classification and relative contribution of the most abundant (> 1 %) sequences  
615 within the *Desulfobacterota* on the surfaces of macrophytes (*C. nodosa* [Mixed Settlement] and *C.*  
616 *cylindracea* [Mixed and Monospecific Settlement]) and in the ambient seawater. The proportion  
617 of sequences classified as *Desulfobacterota* in the total bacterial and archaeal community is given  
618 above the corresponding bar. NR – No Relative

## Jaccard's Similarity Coefficient

<i>Caulerpa cylindracea</i> (Mixed)	0.28		
<i>Caulerpa cylindracea</i> (Monospecific)	0.27	0.35	
Seawater	0.12	0.10	0.10

## Bray-Curtis Similarity Coefficient

	<i>Cymodocea nodosa</i> (Mixed)	<i>Caulerpa cylindracea</i> (Mixed)	<i>Caulerpa cylindracea</i> (Monospecific)
<i>Caulerpa cylindracea</i> (Mixed)	<b>0.40</b>		
<i>Caulerpa cylindracea</i> (Monospecific)	<b>0.38</b>	<b>0.77</b>	
Seawater	<b>0.06</b>	<b>0.05</b>	<b>0.06</b>

**Fig. 1.** Proportion of shared bacterial and archaeal OTUs (Jaccard's Similarity Coefficient) and shared bacterial and archaeal communities (Bray-Curtis Similarity Coefficient) between assemblages associated with the surfaces of macrophytes (*C. nodosa* [Mixed Settlement] and *C. cylindracea* [Mixed and Monospecific Settlement]) and communities in the ambient seawater.

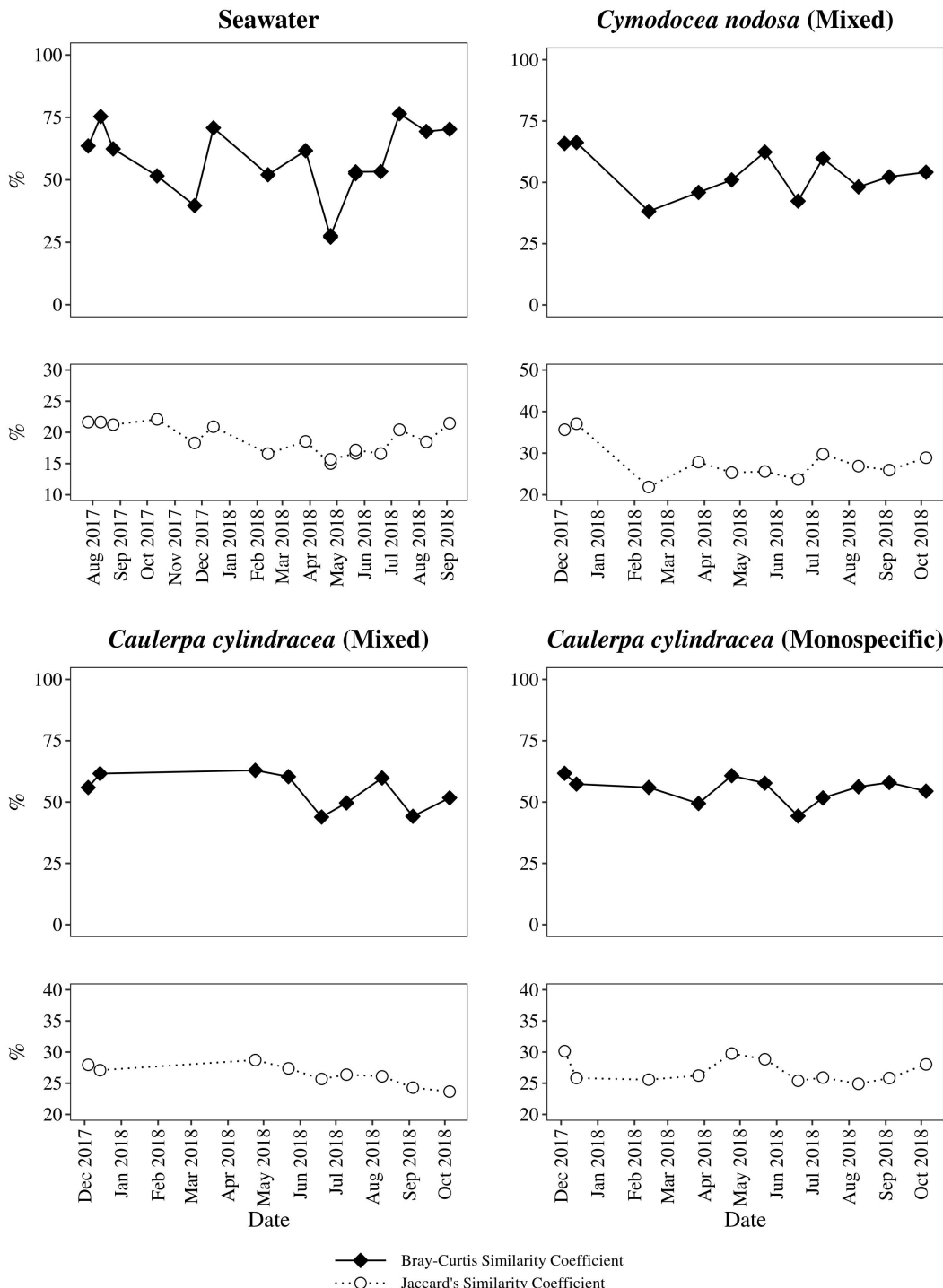


**Fig. 2.** Proportion of shared bacterial and archaeal communities (Bray-Curtis Similarity Coefficient) and shared bacterial and archaeal OTUs (Jaccard's Similarity Coefficient) between consecutive sampling points and from the surfaces of macrophytes (*C. nodosa* [Mixed Settlement] and *C. cylindracea* [Mixed and Monospecific Settlement]) and in the ambient seawater.

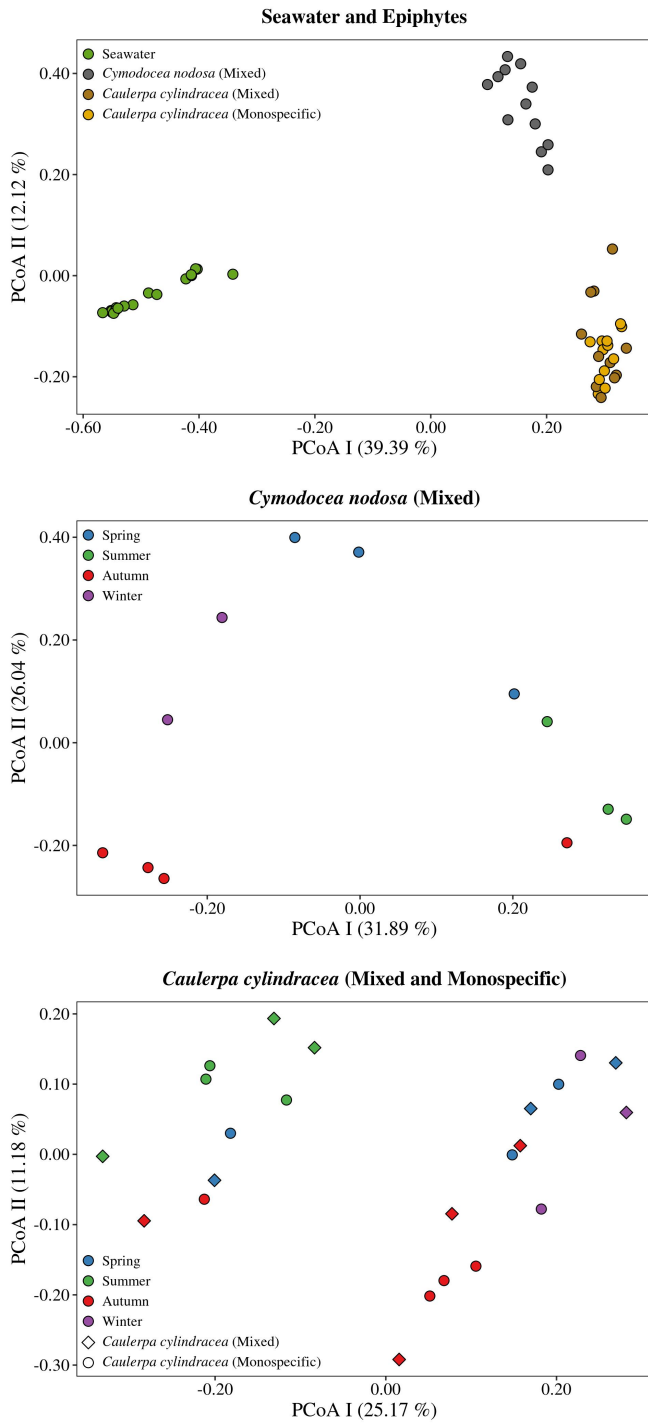


**Fig. 3.** Principal Coordinates Analysis (PCoA) of Bray-Curtis distances based on OTU abundances of bacterial and archaeal communities from the surfaces of macrophytes (*C. nodosa* [Mixed Settlement] and *C. cylindracea* [Mixed and Monospecific Settlement]) and in the ambient seawater. Samples from the same environment or same season are labeled in different colors. The proportion of explained variation by each axis is shown on the corresponding axis in parentheses.

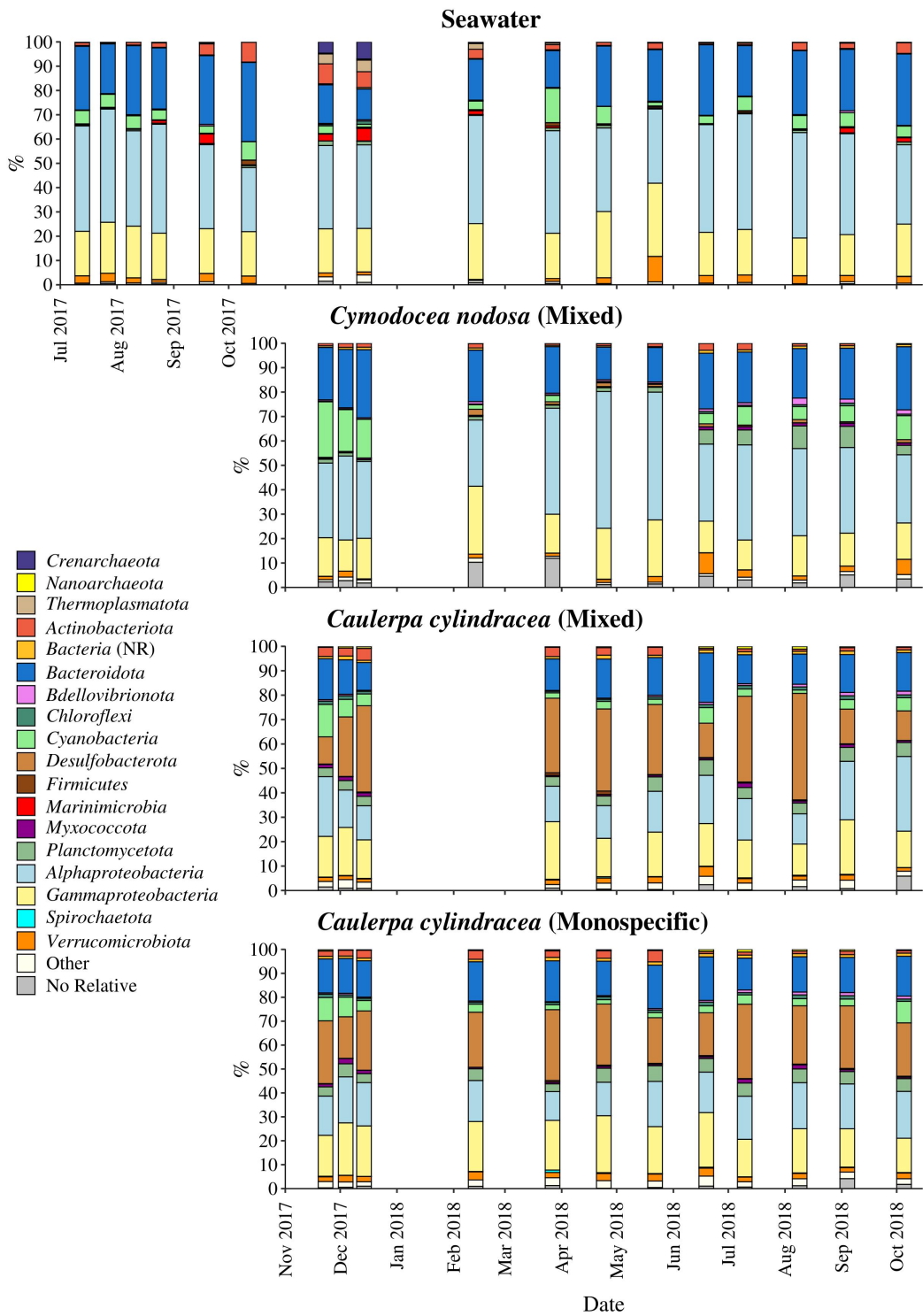


**Fig. 4.** Taxonomic classification and relative contribution of the most abundant (> 1 %) bacterial and archaeal sequences on the surfaces of macrophytes (*C. nodosa* [Mixed Settlement] and *C. cylindracea* [Mixed and Monospecific Settlement]) and in the ambient seawater. NR – No Relative

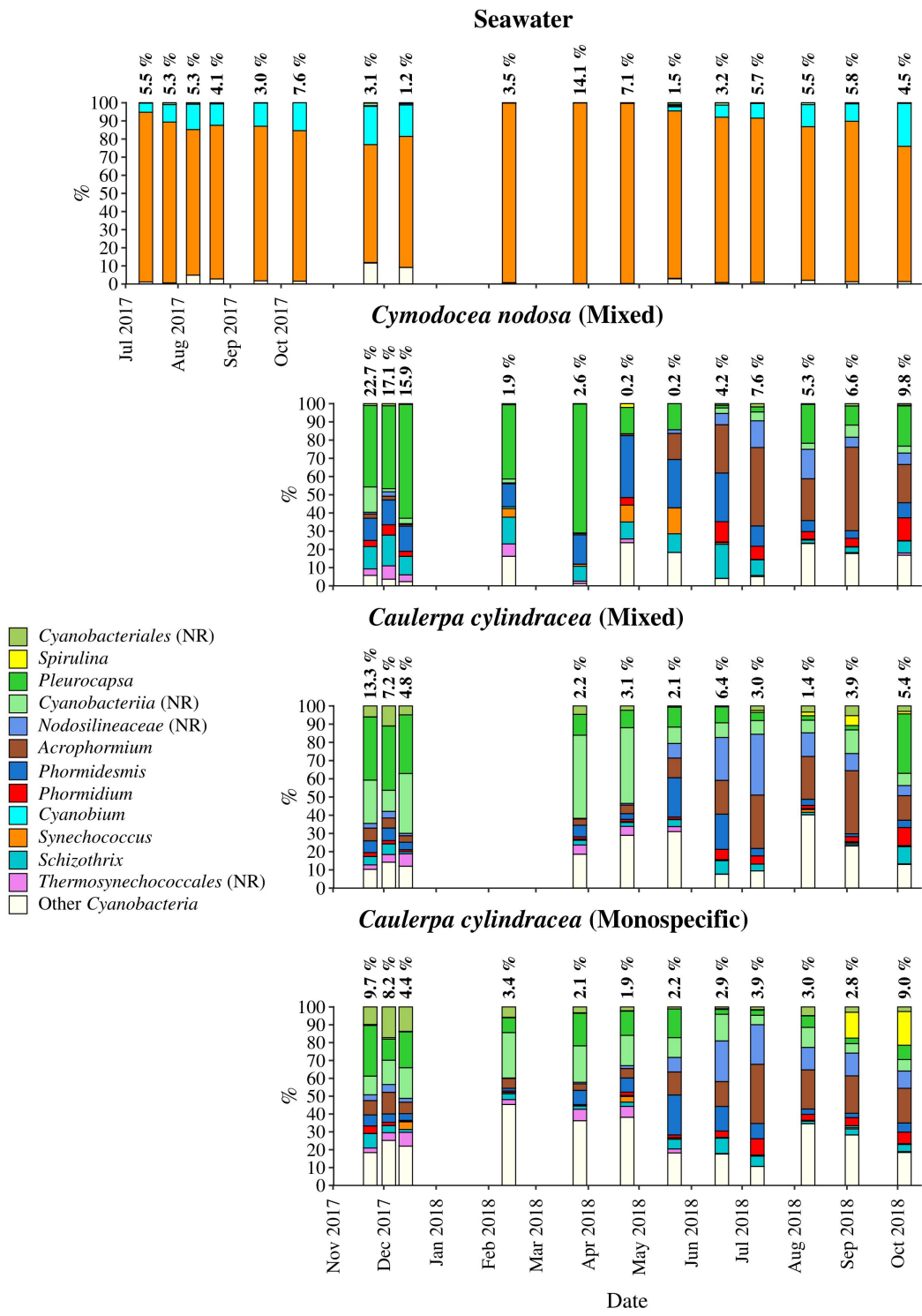


**Fig. 5.** Taxonomic classification and relative contribution of the most abundant (> 1 %) cyanobacterial sequences on the surfaces of macrophytes (*C. nodosa* [Mixed Settlement] and *C. cylindracea* [Mixed and Monospecific Settlement]) and in the ambient seawater. The proportion of cyanobacterial sequences in the total bacterial and archaeal community is given above the corresponding bar. NR – No Relative

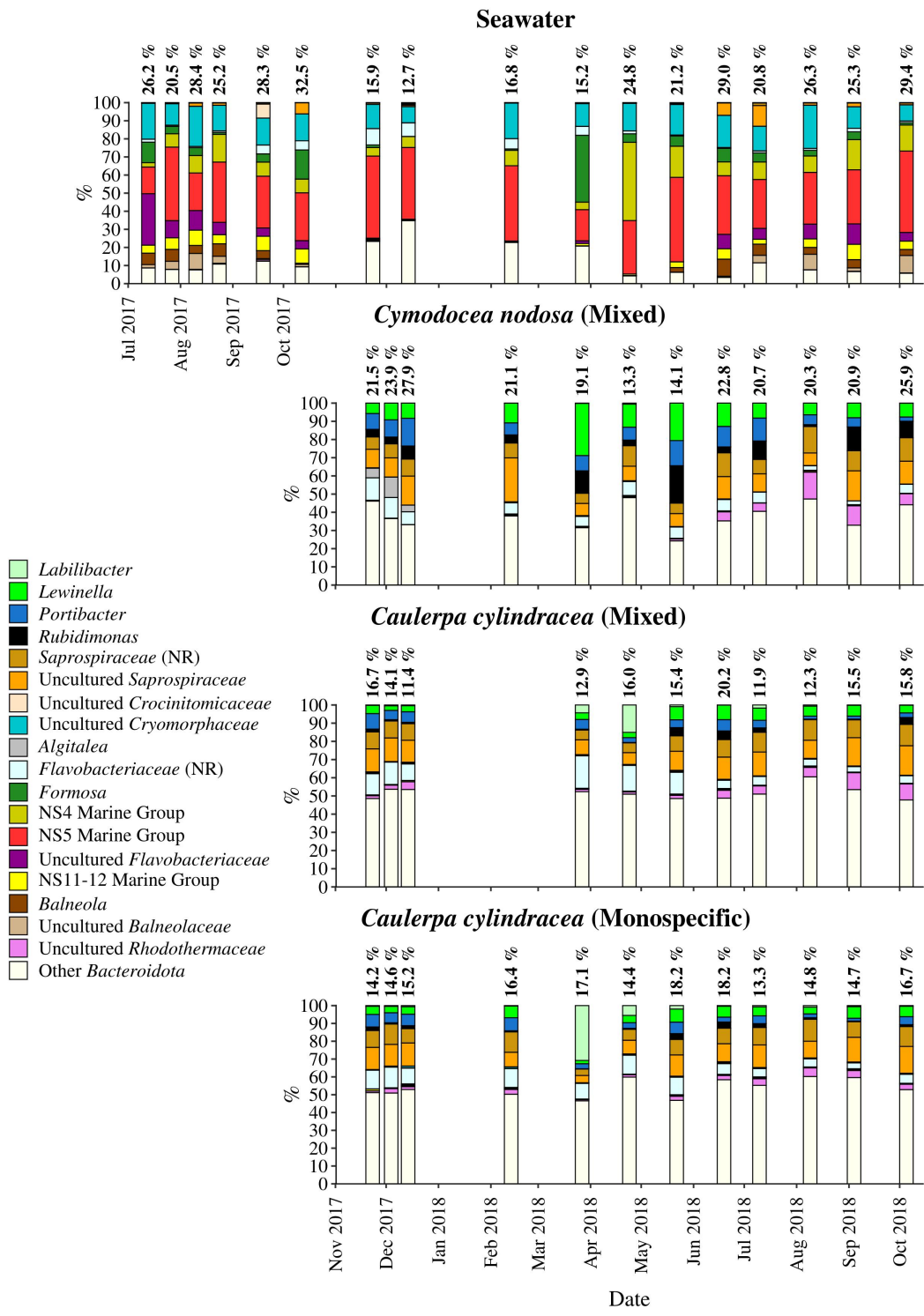


**Fig. 6.** Taxonomic classification and relative contribution of the most abundant (> 2 %) sequences within the *Bacteroidota* on the surfaces of macrophytes (*C. nodosa* [Mixed Settlement] and *C. cylindracea* [Mixed and Monospecific Settlement]) and in the ambient seawater. The proportion of sequences classified as *Bacteroidota* in the total bacterial and archaeal community is given above the corresponding bar. NR – No Relative

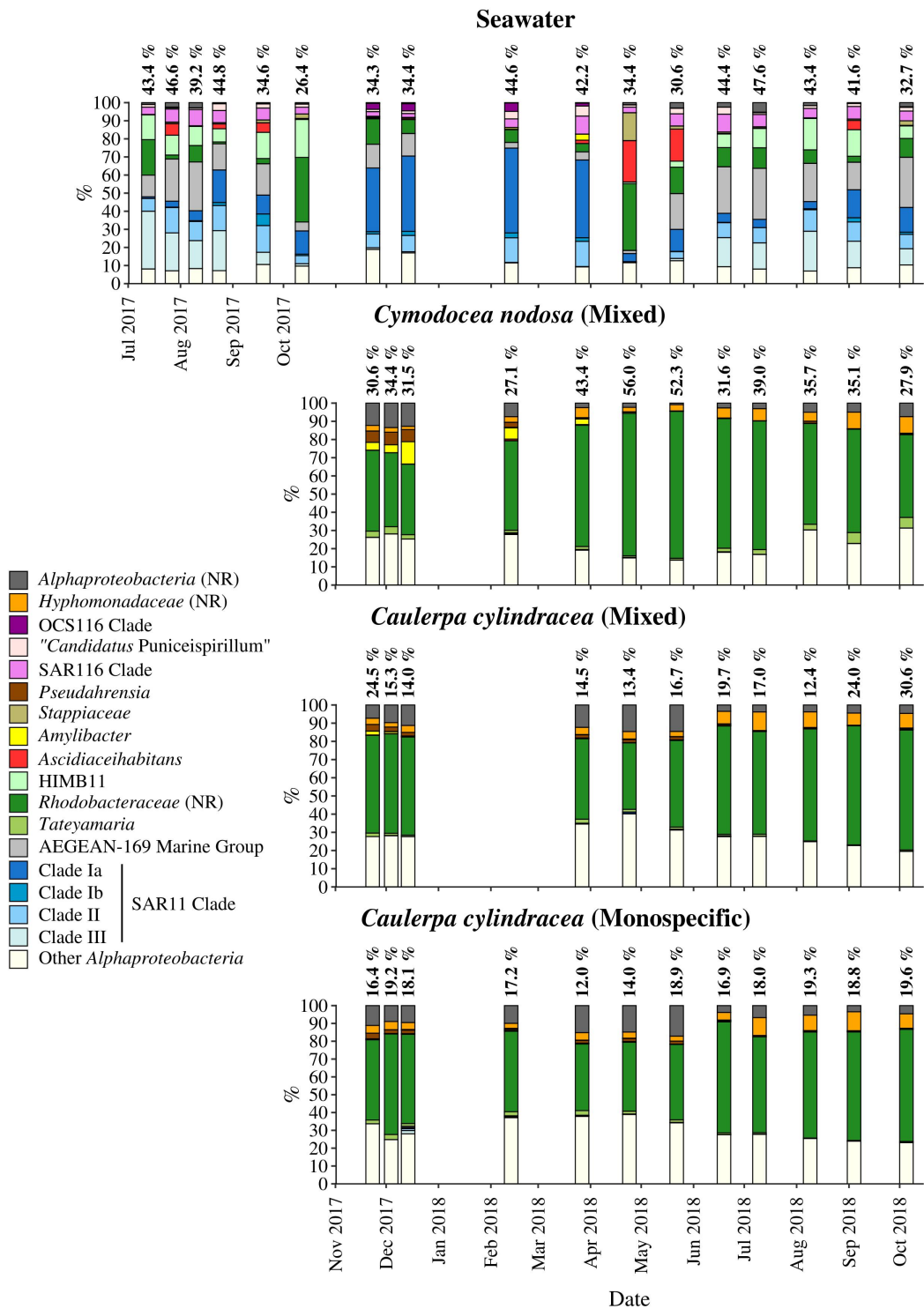


**Fig. 7.** Taxonomic classification and relative contribution of the most abundant (> 2 %) alphaproteobacterial sequences on the surfaces of macrophytes (*C. nodosa* [Mixed Settlement] and *C. cylindracea* [Mixed and Monospecific Settlement]) and in the ambient seawater. The proportion of alphaproteobacterial sequences in the total bacterial and archaeal community is given above the corresponding bar. NR – No Relative

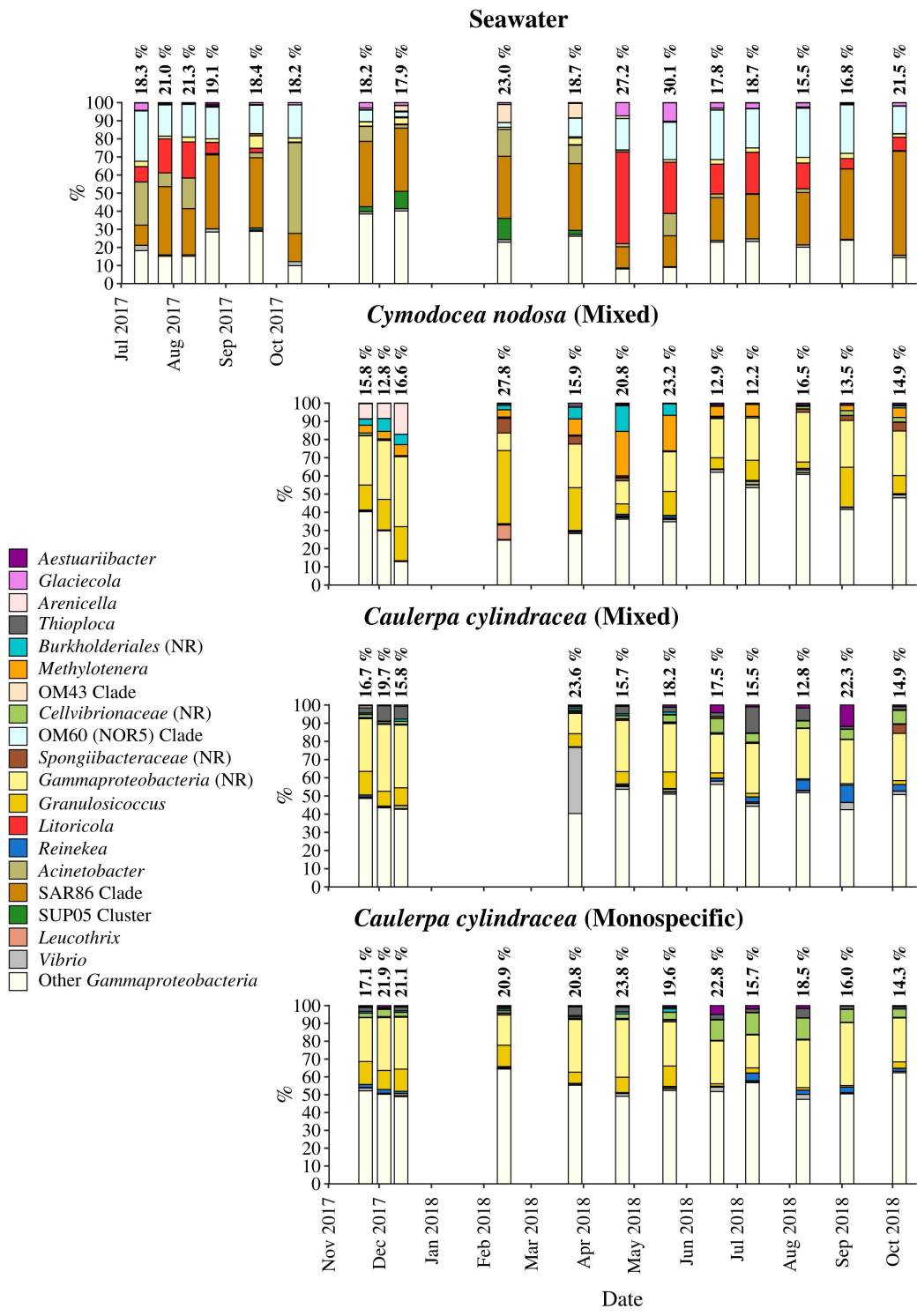


**Fig. 8.** Taxonomic classification and relative contribution of the most abundant (> 2 %) gammaproteobacterial sequences on the surfaces of macrophytes (*C. nodosa* [Mixed Settlement] and *C. cylindracea* [Mixed and Monospecific Settlement]) and in the ambient seawater. The proportion of gammaproteobacterial sequences in the total bacterial and archaeal community is given above the corresponding bar. NR – No Relative

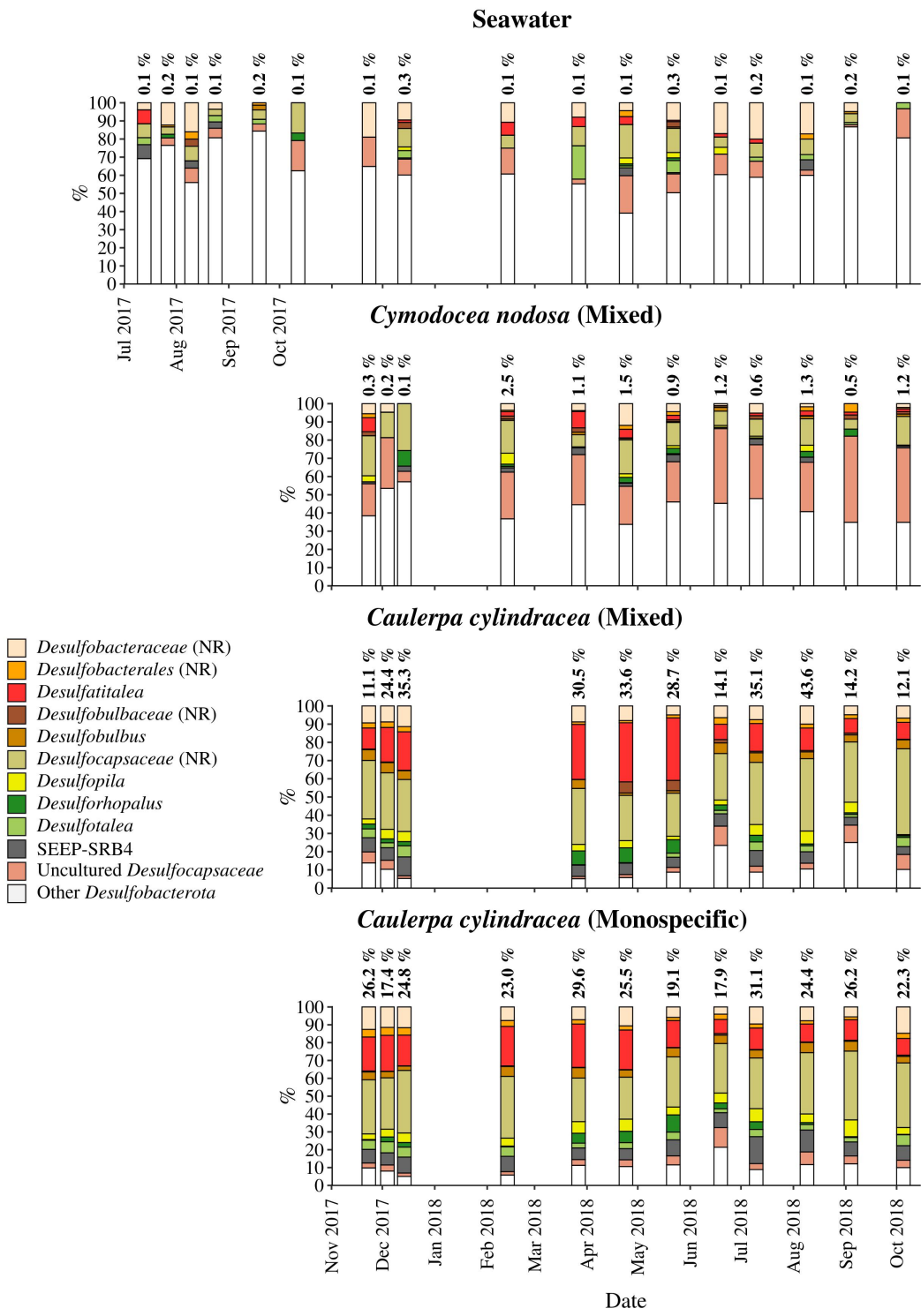


**Fig. 9.** Taxonomic classification and relative contribution of the most abundant (> 1 %) sequences within the *Desulfobacterota* on the surfaces of macrophytes (*C. nodosa* [Mixed Settlement] and *C. cylindracea* [Mixed and Monospecific Settlement]) and in the ambient seawater. The proportion of sequences classified as *Desulfobacterota* in the total bacterial and archaeal community is given above the corresponding bar. NR – No Relative